nature photonics

ARTICLES

PUBLISHED ONLINE: 9 DECEMBER 2012 | DOI: 10.1038/NPHOTON.2012.302

Strain-induced pseudomagnetic field and photonic Landau levels in dielectric structures

Mikael C. Rechtsman[1†]*, Julia M. Zeuner[2†], Andreas Tünnermann[2], Stefan Nolte[2], Mordechai Segev[1] and Alexander Szameit[2]

Magnetic effects at optical frequencies are notoriously weak, so magneto-optical devices must be large to create a sufficient effect. In graphene, it has been shown that inhomogeneous strains can induce 'pseudomagnetic fields' that behave in a similar manner to real ones. Here, we show experimentally and theoretically that it is possible to induce such a field at optical frequencies in a photonic lattice. To our knowledge, this is the first realization of a pseudomagnetic field in optics. The field yields 'photonic Landau levels' separated by bandgaps in the spatial spectrum of the structured dielectric lattice. The gaps between these highly degenerate levels lead to transverse optical confinement. The use of strain allows for the exploration of magnetic-like effects in a non-resonant way that would be otherwise inaccessible in optics. It also suggests the possibility that aperiodic photonic-crystal structures can achieve greater field enhancement and slow-light effects than periodic structures via high density of states at the Landau levels. Generalizing these concepts to systems beyond optics, such as matter waves in optical potentials, offers new intriguing physics that is fundamentally different from that in purely periodic structures.

Magnetism in photonic structures has recently shown promise for a number of applications, despite its fundamentally weak nature at optical frequencies. For example, it has been shown (at microwave frequencies) that gyromagnetic photonic crystals have 'topologically protected' non-reciprocal edge states, meaning that radiation occupying these states is propagating without scattering and is exceedingly robust against disorder[1,2]. A related work[3] has theoretically proposed that a photonic 'topological insulator' structure can be realized using coupled resonator systems[4] for applications in robust delay lines. Optical metamaterials[5], in chiral or nonchiral[6] form, yield induced magnetism at optical frequencies. However, at present, optical metamaterials are extremely lossy, because they incorporate metallic elements and are based on sharp resonances. In contrast, the structure we propose here—a strained honeycomb photonic lattice inspired by carbon-based graphene—contains no metals and is non-resonant, and is therefore loss-free. It exhibits pseudomagnetic effects as a result of the inhomogeneous strain applied to it, which makes it aperiodic. The pseudomagnetism, while not breaking time-reversal symmetry, leads to the generation of discrete photonic Landau levels in the spatial spectrum, which are impossible in a periodic structure. The photonic Landau levels are highly degenerate (and thus have a very high density of states), and gaps form between the Landau levels that lead to transverse spatial confinement of the incident light.

More than a decade ago, Kane and Mele[7] showed that inhomogeneously strained graphene (a honeycomb lattice of carbon atoms) demonstrates a similar physical behaviour to graphene under an added external magnetic field. In particular, engineering a certain inhomogeneous strain to correspond to a constant magnetic field gives rise to Landau levels separated by gaps[8]. Since then, graphene physics has been realized in the optical domain in the form of a honeycomb photonic lattice, which exhibits a similar mathematical description to carbon-based graphene, but with additional effects unique to electromagnetic waves, such as conical diffraction and solitons[9–15]. In the present Article, we demonstrate the existence of pseudomagnetism in such photonic lattices on application of inhomogeneous strain.

A photonic lattice is composed of a periodic array of waveguides that are evanescently coupled to one another. Photonic lattices, which are arranged in a geometry similar to arrays of photonic-crystal fibres[16], have been used in the exploration of a number of fundamental wave-transport phenomena, including discrete solitons[17–20], Anderson localization[21] and edge state properties[22,23]. Figure 1a depicts such a waveguide array, in a honeycomb-lattice configuration that we label 'photonic graphene' with exactly the same geometry as the arrangement of carbon atoms in graphene. As shown, the system is invariant in the z-direction, but arranged as a honeycomb lattice in the transverse (x–y) plane. The propagation of monochromatic light through this waveguide array may be described by coupled-mode equations[20]:

$$i\partial_z \Psi_n = \sum_{<m>} c(|\mathbf{r}_{n,m}|)\Psi_m \qquad (1)$$

where Ψ_n is the amplitude of the mode in the nth waveguide, the summation is taken over all three nearest-neighbour waveguides to the nth, and z is the propagation distance of the light within the photonic lattice. The coupling strength between the waveguides is described by the function $c(r) = c_0 e^{-(r-a)/l_0}$, where a is the nearest-neighbour spacing, l_0 is the coupling decay length, and c_0 is the coupling at $r = a$. Notice that equation (1) is equivalent to the Schrödinger equation in the tight-binding limit. Indeed, it is this analogy between paraxial photonic structures and quantum problems that has given rise to many experimental studies of fundamental issues that would otherwise have been very difficult (sometimes inaccessible) in the quantum world[20,24]. For simplicity, in equation (1) we assume that the waveguides are sufficiently distant from one another that it is only necessary to incorporate nearest-neighbour coupling. Furthermore, it is assumed that each of the

[1]Physics Department, Technion–Israel Institute of Technology, Haifa 32000, Israel, [2]Institute of Applied Physics, Abbe Center of Photonics, Friedrich-Schiller-Universität Jena, Max-Wien-Platz 1, 07743 Jena, Germany, [†]These authors contributed equally to this work. *e-mail: mcrworld@gmail.com

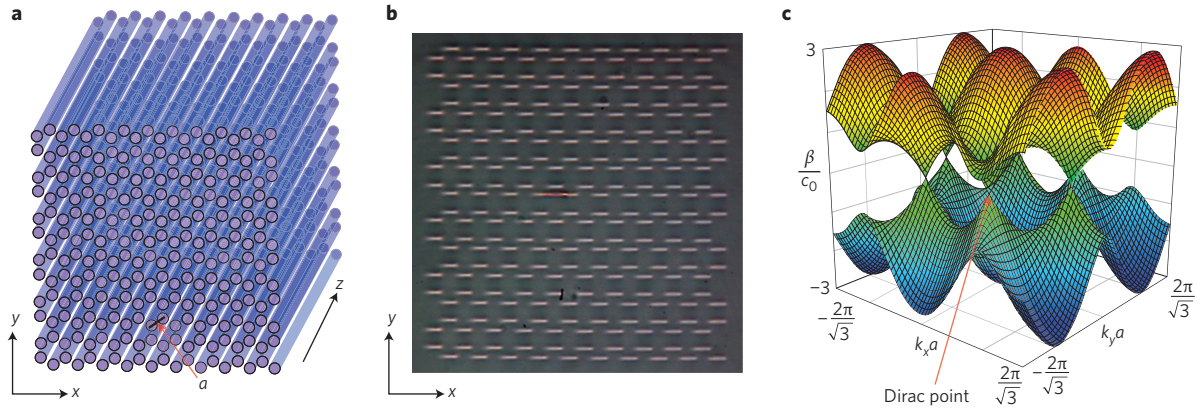

Figure 1 | Description of honeycomb photonic lattice and band structure. a, Diagram of the honeycomb photonic lattice geometry. Light propagates through the structure along the axis of the waveguides (the *z*-axis) by tunnelling between neighbouring waveguides. **b**, Microscope image of the input facet of the photonic lattice geometry. The waveguides are elliptical (due to fabrication constraints), with dimensions of 11 μm in the horizontal direction and 3 μm in the vertical direction. **c**, Band structure diagram of the photonic lattice, with β/c_0 plotted as a function of the Bloch wave vector (k_x,k_y). Note that the first and second bands intersect at the Dirac cones (one of which is indicated by an arrow) that reside at the vertices of the Brillouin zone.

waveguides supports only a single mode. Notice here that the strain makes the coupling vary from site to site, unlike the coupling in uniform lattices where $c(r)$ is simply a constant[17,20]. As noted above, equation (1) is mathematically equivalent to the Schrödinger equation for graphene in the tight-binding limit, where propagation distance z replaces time t. Thus, light that propagates through the photonic lattice diffracts in the z-direction just as electrons in the p orbitals of graphene evolve in time. The transverse wavefunction of the light that emerges from the lattice is therefore equivalent to a finite-time evolution of an electron wavepacket in graphene. As we show below, we demonstrate the presence of a strain-induced magnetic field using this 'time' evolution of light in the photonic lattice.

Our photonic graphene lattice was fabricated using the direct femtosecond laser-writing technique[25] by locally increasing the refractive index to define the waveguides making up the photonic lattice within the volume of a fused-silica sample. A microscope image of the input facet of the photonic lattice is presented in Fig. 1b. Using this fabrication technique, the waveguides are elliptical in nature, with horizontal and vertical diameters of 11 μm and 3 μm, respectively, and the nearest-neighbour spacing is $a = 14$ μm. Specific details of the physical properties of the waveguides used in the experiment are provided in Supplementary Section S1. The guided mode associated with the individual waveguides, as well as its properties, are discussed in Supplementary Section S2. In the experiments, we use laser light at a vacuum wavelength of 633 nm, and the fused-silica sample has a background refractive index of 1.45. By making the substitution $\Psi_n = \psi_n e^{i\beta z}$ in equation (1), where β is the propagation constant, we obtain an eigenvalue equation for the eigenmodes of the system: $-\beta\psi_n = \sum_{<m>} c(|\mathbf{r}_{n,m}|)\psi_m$. Figure 1c presents the band structure of the system, that is, β versus (k_x,k_y), the transverse wavevector. Because the honeycomb lattice has two members in each unit cell, there are two bands (two-dimensional surfaces in Fig. 1c). Note that, conventionally, photonic band structures plot frequency ω versus Bloch wave vector $\mathbf{k}$, whereas Fig. 1c plots β versus (k_x,k_y) at fixed frequency. Accordingly, these bands may be seen as isofrequency contours. The band structure exhibits 'Dirac cones'—conical singularities where the top and bottom bands intersect at a single point. Two of the six Dirac cones shown are mathematically unique, and the others are equivalent to each other through the periodicity of the band structure in (k_x,k_y) space. This band structure of the propagation constant is similar to that of electrons in graphene. Indeed, these similarities have given rise to a variety of ideas that have been carried over from graphene physics to optics and vice versa[10,13,26–28].

It has been shown, for graphene, that for wave packets that lie near a Dirac point, straining the system is mathematically equivalent to introducing magnetic fields[7]. In particular, for a given position-dependent strain tensor $U(\mathbf{r})$, a vector potential $A(\mathbf{r}) = \pm(u_{xx} - u_{yy}, -2u_{xy})/2l_0$ is introduced, where u_{xx}, u_{xy} and u_{yy} are the elements of the two-dimensional strain tensor $U(\mathbf{r})$, and the sign depends on which Dirac point is in question. Note that the expressions for the pseudomagnetic field in graphene and a honeycomb photonic lattice are identical, if we choose units such that $\hbar/e = 1$. Recall that the magnetic field is given by $B(\mathbf{r}) = \nabla \times A(\mathbf{r})$. By choosing a particular form of the strain tensor $U(\mathbf{r})$, it has been demonstrated in graphene[8] that a vector potential corresponding to a constant magnetic field could be achieved, together with a total absence of electric field. In this vein, if the waveguides in our photonic graphene lattice are transversely displaced from their original positions in the following way, then a constant magnetic field is achieved: $(u_r,u_\theta) = qr^2(\sin 3\theta, \cos 3\theta)$, where u_r and u_θ are the radial and azimuthal displacements, r is the distance from an arbitrary origin, θ is the azimuthal angle, and q is a parameter corresponding to the strength of the strain. The result of this displacement is a vector potential $A(\mathbf{r}) = \pm 4q(y, -x)/l_0$, which is in the symmetric gauge and corresponds to a magnetic field of strength $B = 8q/l_0$. Note that the induced pseudomagnetic field does not break z-reversal invariance, just like a pseudomagnetic field in atomic graphene does not break time-reversal symmetry. In other words, the system would behave identically if the photonic lattice were reflected about the $z = 0$ plane. This is because half of the Dirac cones exhibit pseudomagnetic fields in the $+z$ direction, while the other half are in the $-z$ direction[24]. This runs counter to the case of a two-dimensional electron gas with an applied magnetic field, where time-reversal symmetry is broken. In fact, breaking time-reversal symmetry in non-magnetic photonic media requires temporal modulation[29].

When a magnetic field is introduced into a wave equation, Landau levels form in the spectrum. The eigenstates of the system, instead of being spread out over a range of β, congregate at discrete, highly degenerate levels. In the two-dimensional electron gas, Landau levels are directly responsible for the observation of discrete steps in the Hall conductivity, which is known as the quantum Hall effect. In honeycomb photonic lattices, the pseudomagnetic field also separates the spectrum into Landau levels with $\beta = \pm\omega\sqrt{N}$, where $N = 0,1,2,\ldots$ and where $\omega = 3\sqrt{B}c_0 a/2$. The spacing of these Landau levels is unique to honeycomb structures,

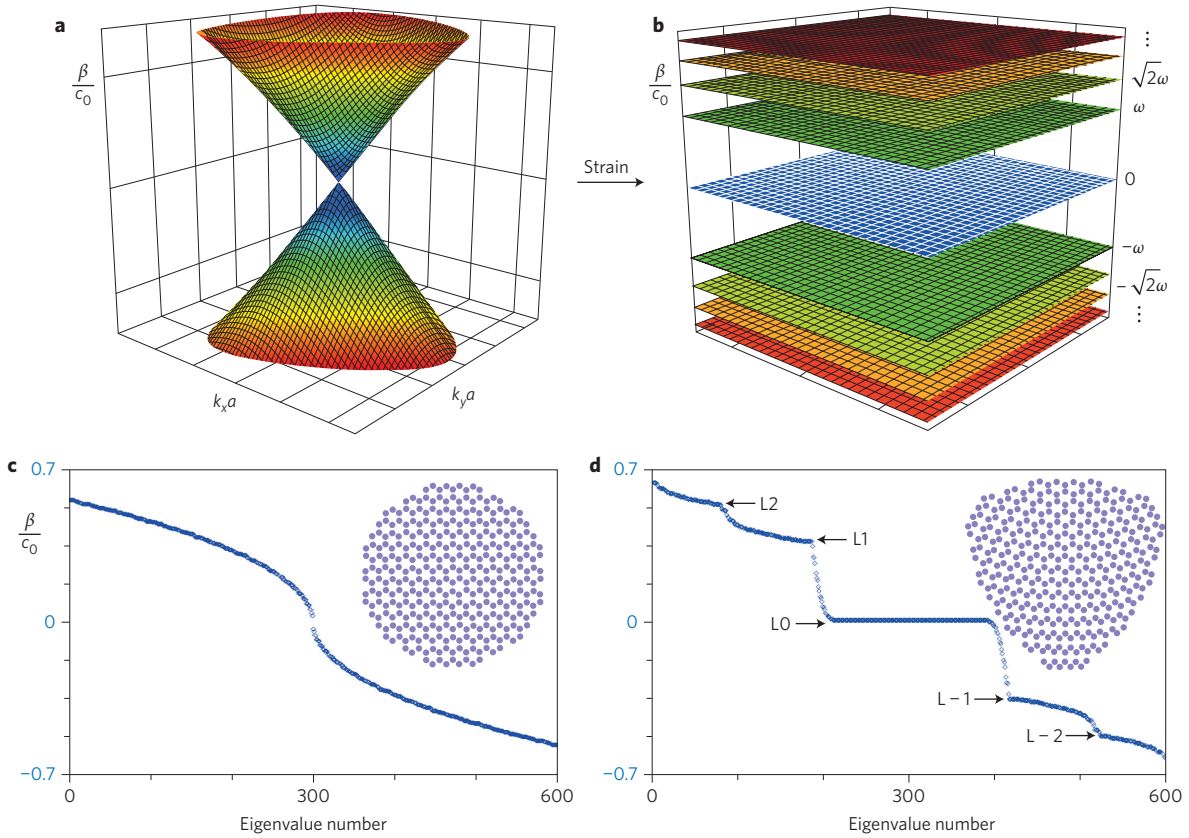

Figure 2 | Effect of strain on the eigenvalue spectrum of the honeycomb photonic lattice. a, Schematic of a Dirac cone in the spectrum of the unstrained honeycomb photonic lattice. **b**, The Dirac cone splits into Landau levels, with $\beta/c_0 = \pm\omega\sqrt{N}$ (where $N = 0,1,2,\ldots$), upon straining the system as described in the text. **c**, Numerically computed eigenvalues plotted in ascending order in the region near the Dirac point for the unstrained lattice. Inset: circular section of the lattice. **d**, Numerically computed eigenvalues for the strained system in the Dirac region, as specified in the text. Inset: effect of strain on the section of the honeycomb lattice shown in **c**. Clear Landau levels emerge in the spectrum as a result of the strain (labelled 'LN'), with edge states lying between them. The calculations for **c** and **d** were carried out for ~9,600 waveguides. The strain in **d** is given by $q = 0.0015a^{-1}$.

and is strongly affected by conical dispersion in the vicinity of the Dirac cones. In two-dimensional electron gases with quadratic dispersion, the Landau levels are equally spaced and do not include the zeroth Landau level[30]. The effect of strain is schematically depicted for an infinite honeycomb lattice in Fig. 2a,b, in a plot showing the spatial spectrum (β versus (k_x,k_y)). Specifically, Fig. 2a shows one of the Dirac cones in an unstrained honeycomb lattice. When the system is properly strained, the states within the Dirac cone split up into highly degenerate Landau levels, with bandgaps lying between them (Fig. 2b). Note that this is an accurate description of the band structure only in the Dirac regions. Outside the Dirac regions, the eigenstates form a continuous band and cannot be described by the pseudomagnetic field. However, in the vicinity of the Dirac points the splitting effect is significant.

To demonstrate numerically the presence of the Landau levels, in Fig. 2c,d we plot the values of β (that is, the spatial spectrum) in the Dirac region for unstrained and strained lattices, in ascending order. Small sections of these finite lattices are shown schematically as insets. For both strained and unstrained lattices, we used a system with ~9,600 waveguides, and for Fig. 2d we used a strain corresponding to $q = 0.0015a^{-1}$ and $l_0 = a/5$. The unstrained system has only armchair-type edges, and no zig-zag or bearded edges[31]. In Fig. 2c, the spectrum for this unstrained system is shown near $\beta/c_0 = 0$, the Dirac region where the Landau levels will emerge upon introducing strain (blue curve). In Fig. 2d, we see that the strain has clearly introduced kinks into the spectrum, which correspond to values of the propagation constant in which many eigenstates reside. These are the Landau levels, and their propagation constants may be calculated, as described above, to be $\beta = \pm 0.37\sqrt{N}c_0$. Note that the numerically calculated positions of the Landau levels coincide exactly with the analytically predicted values (which assume that the states in the vicinity of the Dirac point obey the Dirac equation). The states between the levels are localized solely on the edges of the lattice; that is, these are strictly edge states and are not present in the limit of infinite system size. In the quantum Hall effect, it is these edge states that give rise to Hall conductivity. Furthermore, the strain introduces edge states that are normally associated with zig-zag and bearded edges[31] at $\beta/c_0 = 0$. This is a result of the fact that, although the unstrained lattice may have only armchair edges (which do not have any edge states), in the strained lattice the armchair edge is deformed and therefore may take on some of the character of the other types of edge termination, which have edge states associated with them. As a result, some of the $N = 0$ Landau-level eigenstates have significant power residing on the armchair edges of the sample. The introduction of Landau levels provides a new mechanism, only achievable in aperiodic systems, with which to achieve very high degeneracies (as opposed to the van Hove mechanism typical of photonic crystals and associated with band edges[32]). Therefore, if strain-induced Landau levels can be achieved in a photonic-crystal setting (for example, a photonic-crystal slab on a silicon chip[33], or a three-dimensional photonic crystal[32]), the high density of states can be used for the enhancement of spontaneous emission and nonlinear wave-mixing processes via the Purcell effect[34].

We now proceed to present the observation of a strain-induced pseudomagnetic field in the photonic lattice. To induce the field,

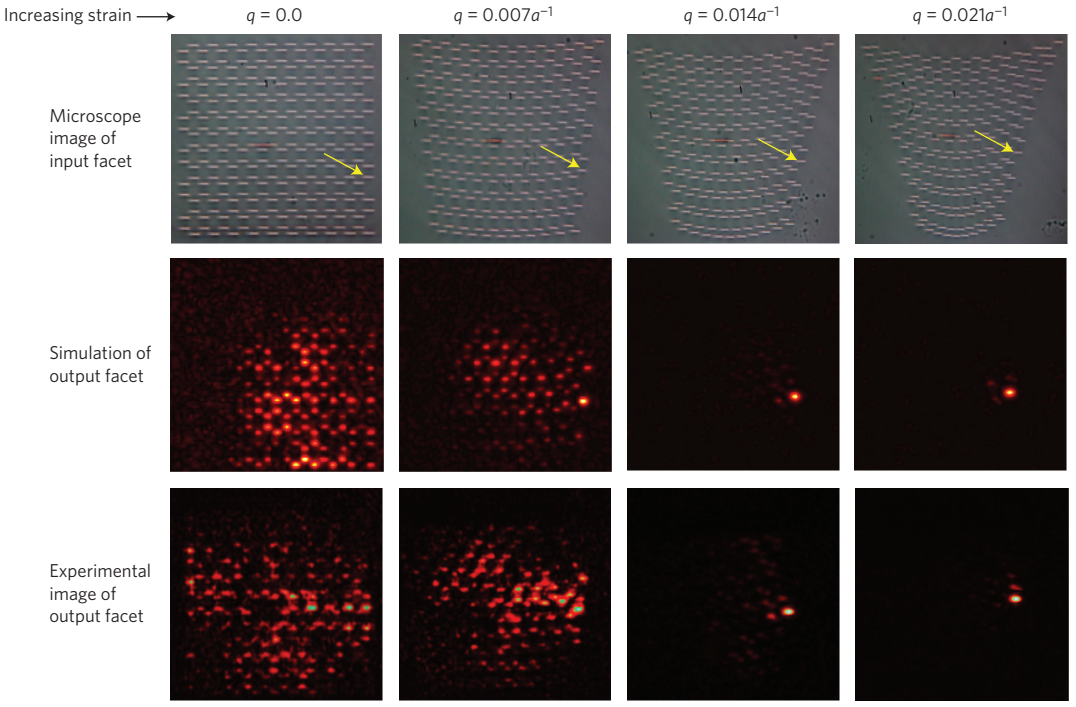

Figure 3 | Experimental and simulation results for increasing strain. Top row: microscope images of the input facet of the lattice. Yellow arrows indicate the waveguide into which the input light beam is launched. This waveguide resides at the armchair edge, which has no edge states. Centre row: simulation results showing the intensity profile at the output facet when light is launched into the edge waveguide (marked by the arrow in the upper row). Bottom row: experimental results showing the intensity profiles of the light exiting the lattice. Results for the unstrained system ($q = 0.0a^{-1}$) are shown in the left-most column. Owing to the lack of edge states on the armchair edge, no light is confined to the edge. The second, third and fourth columns are similar but with successively increasing strains ($q = 0.007a^{-1}$, $0.014a^{-1}$ and $0.021a^{-1}$). Light becomes highly confined on the edge with increasing strain, because the eigenstates excited by the incoming light are either in a bandgap between Landau levels (and therefore cannot penetrate into the bulk) or are degenerate states in the zeroth Landau level, resulting in edge confinement.

we wrote the waveguides at transverse positions that correspond to the inhomogeneous strain described above. A number of different arrays were written to correspond to increasing levels of strain, from $q = 0a^{-1}$ to $q = 0.021a^{-1}$ (where a is the nearest-neighbour distance, as before). If a piece of graphene were strained to this extent, it would yield a pseudomagnetic field of 5,500 T. The top row in Fig. 3 presents optical microscope images of the input facets of our honeycomb photonic lattices, for increasing levels of strain.

We explored the properties of our strained honeycomb photonic lattices using a He–Ne laser (operating at a wavelength of 633 nm) such that light was incident on the input facet of the array and strongly focused on a single waveguide located at the edge of the array. As we will show, there are two reasons why probing the edge of the sample provides a full picture of the nature of the bulk spectrum: (i) it provides a straightforward way of accessing the Dirac region of the spectrum and (ii) the degree of localization on the edge is a clear indicator of whether (or not) the propagation constant of the excited spatial eigenmodes lies in a bulk bandgap between Landau levels. The position of the excited waveguide is marked by an arrow in each of the panels in the upper row of Fig. 3. Because the input beam is focused on a single waveguide, the initial wavefunction is $\Psi_n(z = 0) = \delta_{nl}$, where the beam is incident upon the lth waveguide. Importantly, this input waveguide resides on the armchair edge of the honeycomb lattice, which has no localized states associated with it[31]. Because the unstrained honeycomb lattice does not have edge states on the armchair edge, light starting on that edge immediately spreads away from it into the bulk. This is shown in both the simulations and the experimental results (depicted in the left column, middle and bottom rows of Fig. 3, respectively). As clearly seen in this figure, both the simulations and the experiments show strong beam spreading into the bulk; the minor discrepancies between the exact shapes of the spread beam can be accounted for by uncertainty regarding the precise shape of the individual waveguides comprising the lattice. For larger strains, projecting the initial state of the system (the specific initial beam we use) onto all the eigenstates of the system results in an overlap largely within the Dirac region, as shown in Supplementary Section S3. As the degree of strain q is increased, the light becomes more and more localized on the armchair edge, remaining largely within the same waveguide where it was launched (right column, middle and bottom rows). For sufficiently large strain, light is confined to the edge when the states excited are in a bulk bandgap, and the light attempting to tunnel from the excited-edge waveguide cannot therefore penetrate into the bulk. This strongly indicates the existence of bandgaps lying between Landau levels. As mentioned previously, the strained armchair edge does have edge states associated with it (all lying at propagation constant $\beta/c_0 = 0$; ref. 30 like zig-zag and bearded edge states). As the honeycomb edge states are necessarily degenerate[35] (that is, they all have the same propagation constant), a wave packet made up of a superposition of such states will not spread. In other words, dispersive effects (which would have manifested themselves here as spreading of the beam as it propagates with z) are absent, because all the edge states of this strained honeycomb lattice are degenerate. Accordingly, all acquire phase at the same rate as they propagate, avoiding dispersive effects altogether. Therefore, despite the fact that these edge states are degenerate with the zeroth Landau level and are resonantly coupled to bulk states, they do not couple into the bulk, and the light is therefore confined

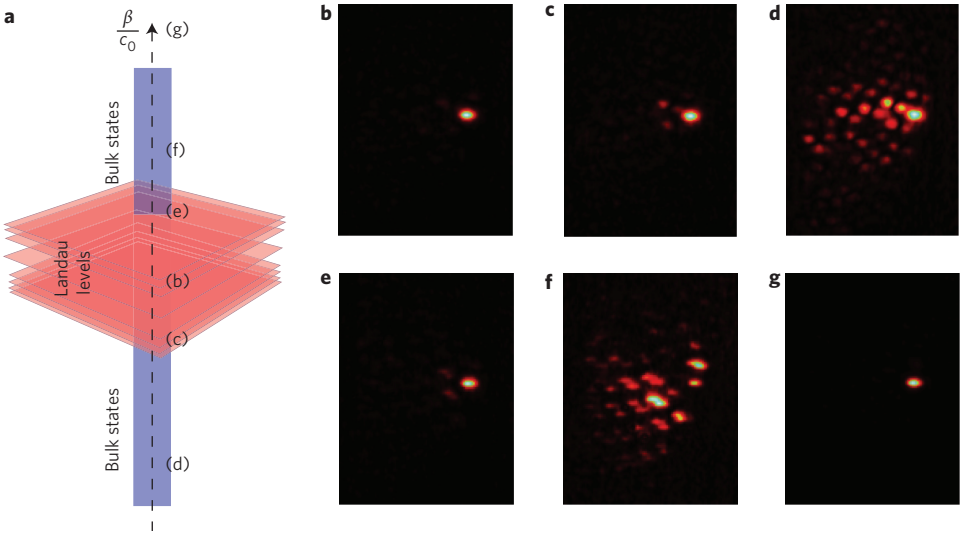

Figure 4 | Effect of a defect waveguide on beam confinement. a, Schematic of the eigenvalue spectrum of a strained honeycomb photonic lattice. Landau levels reside at the centre, where the Dirac cones lie. **b**, Experimental results showing the light exiting the strained lattice when a single waveguide on the armchair edge is excited. The light is confined as a result of the gaps between the Landau levels, as described in the text and as shown in Fig. 3. **c**, Light exiting the strained lattice when the excited waveguide is engineered to have a slightly negative defect ($\beta_l/c_0 = -0.5$). As a result, coupling with the bulk bands causes some spreading. **d**, Larger defect strengths ($\beta_l/c_0 = -2$) cause more spreading. **e**, A mildly positive defect ($\beta_l/c_0 = 0.5$) also causes some spreading, as in **c**. **f**, A stronger positive defect ($\beta_l/c_0 = 2$) causes greater spreading (as in **d**) as a result of strong coupling to the bulk bands. **g**, Once the defect mode is very strong ($\beta_l/c_0 = 4$) it becomes a defect mode outside of the band and therefore in another bandgap. As a result, it becomes localized again. These results, taken together, locate the excitation of the defect-free case ($\beta_l/c_0 = 0$) within the Landau level gaps.

on the edge. In summary, the strain leads to confinement for two reasons. First, the initial beam excites states in the gap between Landau levels, which are confined to the edge. Second, the initial beams excite degenerate edge states in the zeroth Landau level, which cannot cause diffraction because of their degeneracy. In the following, we show that the excited eigenmodes indeed reside in the Dirac region at the centre of the spectrum.

It is essential to prove that the lack of tunnelling from the waveguide residing on the armchair edge into the bulk indeed arises from the presence of the gaps between Landau levels, and not from some coincidental perturbation near the edge that would constitute a simple 'defect mode'. To show this, we fabricated several different samples, all with a given strain $q = 0.021a^{-1}$, with the waveguide we excite replaced by a 'defect waveguide'. Specifically, we changed the refractive index of that waveguide (while leaving all others fixed), such that it was higher or lower than the others. When a defect mode is introduced, equation (1) must be changed to

$$i\partial_z \Psi_n + \beta_l \delta_{nl} \Psi_n = \sum_{<m>} c(|\mathbf{r}_{nm}|)\Psi_m$$

where β_l is the intrinsic propagation constant of the defect waveguide mode. The dimensionless parameter β_l/c_0 describes the strength of the defect mode: it is positive if the change in refractive index is positive and negative if the change in refractive index is negative. Intuitively, changing the refractive index of the defect waveguide is akin to changing the depth of the 'potential well' associated with that waveguide, which in turn allows tuning of β throughout the spectrum. By tuning the mean excited propagation constant in this way, we target a particular region of the spatial spectrum. Details of the calculation of β_l/c_0 for a defect waveguide of given propagation constant are presented in Supplementary Section S2. We schematically depict the nature of the entire band structure of the strained honeycomb lattice in Fig. 4a. In the centre (near the Dirac cone regions) lie the Landau levels (symmetric on either side of $\beta = 0$). On either side of the Landau levels lie the eigenstates of the photonic lattice, which are outside the Dirac region. These regions are largely composed of bulk eigenstates that penetrate throughout the lattice. In Fig. 4b, we show the output facet of the lattice where there is no defect ($\beta_l/c_0 = 0$): light is tightly confined because it has excited localized eigenstates lying within Landau-level gaps that are localized near the edge of the lattice. On slightly decreasing the refractive index of the defect waveguide (such that $\beta_l/c_0 = -0.5$), shown in Fig. 4c, the beam at the output facet expands slightly, reflecting the increasing overlap with the continuum modes below the Landau levels in the band structure. On strongly decreasing the refractive index of the waveguide ($\beta_l/c_0 = -2$), the excited eigenstates are bulk states, well away from the Landau levels, so light significantly spreads into the bulk of the structure (Fig. 4d). We now consider defect waveguides with a refractive index larger than the ambient index of the remainder of the waveguides. Just as in the negative defect case, a slight increase in the refractive index, corresponding to $\beta_l/c_0 = 0.5$, leads to a slight increase in the expansion of the beam by the time it gets to the output facet of the lattice (Fig. 4e). However, a much stronger increase, corresponding to $\beta_l/c_0 = 2$, shows a dramatic expansion of the beam because the excited eigenstates (which are spectrally distant from the Dirac region where the Landau levels reside) now lie throughout the bulk of the photonic lattice (Fig. 4f). A further increase in the refractive index (such that $\beta_l/c_0 = 4$) results in relocalization of the beam (Fig. 4g). The reason why the beam relocalizes for a sufficiently strong refractive index is that the defect eigenstate has passed through the entire band and now lies above it, acting much like a localized donor or acceptor mode in a semiconductor. Outside the band, the state resides in a bandgap (although not one induced by the strain), and thus cannot overlap with any modes that spread throughout the bulk of the photonic lattice. The fact that both the negative and positive defects lead to spreading strongly indicates that the gap between strain-induced Landau levels lies at the centre of the band in the Dirac region.

The introduction of strong magnetic effects in optical systems opens the door to a wide range of new physical effects and

applications. For example, recent work on gyrotropic photonic crystals[2] has shown, in the microwave regime, that quantum Hall physics may be used to achieve scatter-free propagation in optical isolators. The fact that the pseudomagnetic field has the effect of 'grouping' eigenstates together into highly degenerate Landau levels suggests the possibility of using this effect for extreme efficiency enhancement in nonlinear devices in photonic crystals. Fundamental questions remain to be answered. For example, can a pseudomagnetic field be observed using strain in a photonic-crystal slab geometry (that is, a two-dimensional geometry with a finite height in the third direction) to utilize the field on a silicon chip? Can this high density of states be engineered by strain in a fully three-dimensional photonic crystal? What is the nonlinear enhancement associated with Landau levels? The strained photonic lattice provides an excellent experimental setting for probing both linear and nonlinear effects of magnetism in optics. Furthermore, the recent observation of parity-time (PT) symmetry breaking in optics[36,37] has very intriguing implications in honeycomb PT-symmetric lattices[11,38], which suggests that the strained honeycomb lattice may provide a context for understanding the effect of magnetism on the PT transition, and on non-Hermitian optics in general[12,39,40]. Can terahertz generation be enhanced in photonic crystals via strain? What is the nature of wave-mixing processes between highly degenerate Landau levels? Can lasing thresholds in photonic crystals be reduced via pseudomagnetic fields? In the plethora of applications where structured photonics have an important technological impact, a new important question will be 'Can we make them better via an inhomogeneous strain?'

Received 17 July 2012; accepted 29 October 2012; published online 9 December 2012

References

1. Haldane, F. D. M. & Raghu, S. Possible realization of directional optical waveguides in photonic crystals with broken time-reversal symmetry. *Phys. Rev. Lett.* **100,** 013904 (2008).
2. Wang, Z., Chong, Y., Joannopoulos, J. D. & Soljačić, M. Observation of unidirectional backscattering-immune topological electromagnetic states. *Nature* **461,** 772–775 (2009).
3. Hafezi, M., Demler, E. A., Lukin, M. D. & Taylor, J. M. Robust optical delay lines with topological protection. *Nature Phys.* **7,** 907–912 (2011).
4. Yariv, A., Xu, Y., Lee, R. K. & Scherer, A. Coupled-resonator optical waveguide: a proposal and analysis. *Opt. Lett.* **24,** 711–713 (1999).
5. Cai, W. & Shalaev, V. *Optical Metamaterials: Fundamentals and Applications* (Springer, 2009).
6. Plum, E. *et al.* Metamaterials: optical activity without chirality. *Phys. Rev. Lett.* **102,** 113902 (2009).
7. Kane, C. L. & Mele, E. J. Size, shape, and low energy electronic structure of carbon nanotubes. *Phys. Rev. Lett.* **78,** 1932–1935 (1997).
8. Guinea, F., Katsnelson, M. I. & Geim, A. K. Energy gaps and a zero-field quantum Hall effect in graphene by strain engineering. *Nature Phys.* **6,** 30–33 (2010).
9. Peleg, O. *et al.* Conical diffraction and gap solitons in honeycomb photonic lattices. *Phys. Rev. Lett.* **98,** 103901 (2007).
10. Bahat-Treidel, O., Peleg, O. & Segev, M. Symmetry breaking in honeycomb photonic lattices. *Opt. Lett.* **33,** 2251–2253 (2008).
11. Bahat-Treidel, O. & Segev, M. Nonlinear wave dynamics in honeycomb lattices. *Phys. Rev. A* **84,** 021802(R) (2011).
12. Szameit, A., Rechtsman, M. C., Bahat-Treidel, O. & Segev, M. PT-symmetry in honeycomb photonic lattices. *Phys. Rev. A* **84,** 021806(R) (2011).
13. Ablowitz, M. J., Nixon, S. D. & Zhu, Y. Conical diffraction in honeycomb lattices. *Phys. Rev. A* **79,** 053830 (2009).
14. Soljačić, M. & Joannopoulos, J. D. Enhancement of nonlinear effects using photonic crystals. *Nature Mater.* **3,** 211–219 (2004).
15. Molina, M. I. & Kivshar, Y. S. Discrete and surface solitons in photonic graphene nanoribbons. *Opt. Lett.* **35,** 2895–2897 (2010).
16. Birks, T. A., Knight, J. C. & Russell, P. S. J. Endlessly single-mode photonic crystal fiber. *Opt. Lett.* **22,** 961–963 (1997).
17. Christodoulides, D. N. & Joseph, R. I. Discrete self-focusing in nonlinear arrays of coupled waveguides. *Opt. Lett.* **13,** 794–796 (1988).
18. Fleischer, J. W., Segev, M., Efremidis, N. K. & Christodoulides, D. N. Observation of two-dimensional discrete solitons in optically induced nonlinear photonic lattices. *Nature* **422,** 147–150 (2003).
19. Eisenberg, H. S., Silberberg, Y., Morandotti, R., Boyd, A. R. & Aitchison, J. S. Discrete spatial optical solitons in waveguide arrays. *Phys. Rev. Lett.* **81,** 3383–3386 (1998).
20. Lederer, F. *et al.* Discrete solitons in optics. *Phys. Rep.* **463,** 1–126 (2008).
21. Schwartz, T., Bartal, G., Fishman, S. & Segev, M. Transport and Anderson localization in disordered two-dimensional photonic lattices. *Nature* **446,** 52–55 (2007).
22. Makris, K. G., Suntsov, S., Christodoulides, D. N., Stegeman, G. I. & Hache, A. Discrete surface solitons. *Opt. Lett.* **30,** 2466–2468 (2005).
23. Malkova, N., Hromada, I., Wang, X., Bryant, G. & Chen, Z. Observation of optical Shockley-like surface states in photonic superlattices. *Opt. Lett.* **34,** 1633–1635 (2009).
24. Longhi, S. Quantum-optical analogies using photonic structures. *Laser Photon. Rev.* **3,** 243–261 (2009).
25. Szameit, A. & Nolte, S. Discrete optics in femtosecond-laser-written photonic structures. *J. Phys. B* **43,** 163001 (2010).
26. Bahat-Treidel, O. *et al.* Klein tunneling in deformed honeycomb lattices. *Phys. Rev. Lett.* **104,** 063901 (2010).
27. Sepkhanov, R. A., Bazaliy, Y. B. & Beenakker, C. W. J. Extremal transmission at the Dirac point of a photonic band structure. *Phys. Rev. A* **75,** 063813 (2007).
28. Bravo-Abad, J., Joannopoulos, J. D. & Soljačić, M. Enabling single-mode behavior over large areas with photonic Dirac cones. *Proc. Natl Acad. Sci. USA* **109,** 9761–9765 (2012).
29. Yu, Z. & Fan, S. Complete optical isolation created by indirect interband photonic transitions. *Nature Photon.* **3,** 91–94 (2009).
30. Stone, M. *Quantum Hall Effect* (World Scientific, 1992).
31. Kohmoto, M. & Hasegawa, Y. Zero modes and edge states of the honeycomb lattice. *Phys. Rev. B* **76,** 205402 (2007).
32. Lodahl, P. *et al.* Controlling the dynamics of spontaneous emission from quantum dots by photonic crystals. *Nature* **430,** 654–657 (2004).
33. Johnson, S. G., Fan, S., Villeneuve, P. R., Joannopoulos, J. D. & Kolodziejski, L. A. Guided modes in photonic crystal slabs. *Phys. Rev. B* **60,** 5751–5758 (1999).
34. Purcell, E. Spontaneous emission probabilities at radio frequencies. *Phys. Rev.* **69,** 681 (1946).
35. Akhmerov, A. R. & Beenakker, C. W. J. Boundary conditions for Dirac fermions on a terminated honeycomb lattice. *Phys. Rev. B* **77,** 085423 (2008).
36. Ruter, C. E. *et al.* Observation of parity-time symmetry in optics. *Nature Phys.* **6,** 192–195 (2010).
37. Guo, A. *et al.* Observation of PT-symmetry breaking in complex optical potentials. *Phys. Rev. Lett.* **103,** 093902 (2009).
38. Kottos, T. Optical physics: broken symmetry makes light work. *Nature Phys.* **6,** 166–167 (2010).
39. Makris, K. G., El-Ganainy, R., Christodoulides, D. N. & Musslimani, Z. H. Beam dynamics in PT symmetric optical lattices. *Phys. Rev. Lett.* **100,** 103904 (2008).
40. Klaiman, S., Günther, U. & Moiseyev, N. Visualization of branch points in PT-symmetric waveguides. *Phys. Rev. Lett.* **101,** 080402 (2008).

Acknowledgements

M.C.R. acknowledges the Azrieli Foundation for the award of an Azrieli fellowship. A.S. acknowledges support from the German Ministry of Education and Research (Center for Innovation Competence programme, grant 03Z1HN31). M.S. acknowledges support from the Israel Science Foundation, the USA–Israel Binational Science Foundation, and the Advanced Grant by the European Research Council.

Author contributions

M.C.R. and J.M.Z. contributed equally. All authors contributed significantly.

Additional information

Supplementary information is available in the online version of the paper. Reprints and permission information is available online at http://www.nature.com/reprints. Correspondence and requests for materials should be addressed to M.C.R.

Competing financial interests

The authors declare no competing financial interests.